Catalysis Today 164 (2011) 92–99

Contents lists available at ScienceDirect

Catalysis Today

journal homepage: www.elsevier.com/locate/cattod

Geopolymer based catalysts—New group of catalytic materials

Petr Sazama[a,*], Oleg Bortnovsky[b], Jiří Dědeček[a], Zdenka Tvarůžková[a], Zdeněk Sobalík[a]

[a] *J. Heyrovský Institute of Physical Chemistry, Academy of Sciences of the Czech Republic, v. v. i., CZ-182 23 Prague 8, Czech Republic*
[b] *Research Institute of Inorganic Chemistry, Unipetrol a.s., Revoluční 84, Ústí n. Labem CZ-400 01, Czech Republic*

ARTICLE INFO

Article history:
Available online 16 October 2010

Keywords:
Geopolymers
Redox catalysis
SCR–NO_x
Catalytic oxidation of VOC

ABSTRACT

New type of redox heterogeneous catalysts based on geopolymer aluminosilicate materials was developed and their catalytic properties have been demonstrated on industrially important reactions. Geopolymers can be regarded as amorphous analogues of zeolitic materials (three dimensional network of SiO_4 and AlO_4 tetrahedra with negative charge of the network balanced by extra-framework cations, variability in chemical composition, ion exchange properties, presence of rings forming cationic sites for bare cations), but possessing some advantages as network formation at ambient or low temperatures, mesoporosity and low cost preparation. It is shown that the geopolymer network enables incorporation of transition metal ions as active centres for catalytic reactions. The catalytic activity of geopolymer-based catalysts with Fe, Co and Cu metal ions in extra-network sites and Pt species is demonstrated on the selective catalytic reduction of nitrogen oxides by ammonia and the total oxidation of volatile hydrocarbons. These findings open a potential for synthesis of new types of robust catalysts for heterogeneously catalysed reactions.

1. Introduction

The term geopolymer, introduced by Davidovits in 1979, represents inorganic materials usually prepared using reactions of various aluminosilicates with hydroxides, carbonates or silicates of alkali and alkaline earth metals. The synthesis yields an amorphous or semi-crystalline monolithic material with three-dimensional network of AlO_4 and SiO_4 tetrahedra connected by oxygen corners exhibiting high strength and resistance to high temperatures, chemicals, etc. [1,2]. This results in the application of geopolymers in building industry, for solidification of hazardous chemicals, and for sophisticated applications as composites materials, adsorbents of cations from waste water, etc. as it has been reported in Refs. [1,3–7]. The basis for same of these applications is interaction of cationic species of transient metals with geopolymers resulting in immobilization of the cations. In contrast to crystalline aluminosilicates, the synthesis of geopolymers proceeds at ambient or slightly elevated temperatures and atmospheric pressure and the whole volume of the synthetic mixture undergoes hardening. Alkaline activation with subsequent polymerization in the whole volume resulting in three dimensional network differentiates geopolymers from amorphous aluminosilicates. Due to the absence of long-range ordering, the structure of geopolymers is not well known. Davidovits suggested their structure as an analogy to organic polymers based on linear hydrocarbons [1,8]. Recent progress in the analysis of geopolymers indicates that these materials should probably be regarded as amorphous analogues of zeolites [9,10]. The negative charge of the network resulting from the presence of AlO_4 tetrahedra in the silicate framework is balanced by extra-framework cations, typically Na(I) or K(I). SiO_4 and AlO_4 tetrahedra are arranged to form rings with variable size. It has been suggested that deformed six-, eight- and ten-membered rings are present in the geopolymer network. Such an arrangement results in properties similar to those of zeolites: (i) All extra-framework cations can be replaced by different ones (ion exchange) [10]. (ii) Bare cations can be located in a dehydrated geopolymer at cationic sites. It has been suggested that six or eight-membered rings accommodate bare divalent cations. [10]. (iii) At least part of cations located at extra-framework sites is accessible for reactants [10]. (iv) Ion exchange of a geopolymer with a solution of an NH_4^+ salt followed by deammonization of a NH_4-geopolymer at elevated temperature or equilibration of the cationic form of a geopolymer with a diluted acid results in the formation of the acidic H-form of the geopolymer.

The close similarity of the geopolymer network and the zeolite framework in relation to ion exchange and accommodation of metal ions opens questions on possibilities for the application of geopolymer materials as amorphous analogues of zeolites. Catalytic properties of metal/metal–oxo cationic species located in zeolites in redox reactions are well known and they are employed in several industrial catalysts mainly for deNO_x processes [11]. We have

---

[*] Corresponding author.
E-mail address: petr.sazama@jh-inst.cas.cz (P. Sazama).

0920-5861/$ – see front matter © 2010 Elsevier B.V. All rights reserved.
doi:10.1016/j.cattod.2010.09.008

Table 1
List of used geopolymer based catalyst.

Sample	Preparation method	Catalytic reaction
Na-Geo-1	Metakaolin-based Na-geopolymer	Parent geopolymer
KCa-Geo-2	Metakaolin-slag-based K-geopolymer	Parent geopolymer
NH_4-Geo-1	Ion exchange of Na-Geo-1 with NH_4NO_3 solution	Selective catalytic reduction of NO_x by NH_3
$CuNH_4$-Geo-1	Ion exchange of NH_4-Geo-1 with $Cu(NO_3)_2$ solution	Selective catalytic reduction of NO_x by NH_3
$CuNH_4$-Geo-2	Ion exchange of NH_4-Geo-2 with $Cu(NO_3)_2$ solution	Selective catalytic reduction of NO_x by NH_3
$PtNH_4$-Geo-2	Ion exchange of NH_4-Geo-2 with $Pt[(NH_3)_4Cl_2]$ solution	Total oxidation of decane as VOC
FeKCa-Geo-2	Impregnation of KCa-Geo-2 with solution of $FeCl_3$ in acetyl acetone	Total oxidation of decane as VOC
$CoNH_4$-Geo-2	Ion exchange of NH_4-Geo-2 with $Co(NO_3)_2$ solution	Total oxidation of decane as VOC

reported the use of geopolymers or modified geopolymer materials in catalytic processes [12,13], however it has not been discussed in opened literature.

The present work is concerned with the synthesis and application of new types of geopolymer materials with incorporated Co, Cu, Fe and Pt species with possible catalytic properties. Catalytic reduction of nitrogen oxides by ammonia and catalytic oxidation of VOCs as industrially important, heterogeneously catalysed reactions were selected to test the catalytic properties of geopolymer catalysts.

2. Experimental

2.1. Preparation of geopolymer catalysts

Table 1 lists the parent geopolymers and geopolymer catalysts used in this study. Parent Na-Geo-1 geopolymer with sodium as a charge compensating cation, was prepared by mixing of 10 g metakaolin (43.5 wt.% of Al_2O_3 and 53.7 wt.% of SiO_2) with an alkali activator containing 12.2 g of water glass (32.0 wt.% of SiO_2, 17.7 wt.% of Na_2O; molar ratio SiO_2/Na_2O of 1.9) and 1.1 g of NaOH (49.4 wt.% in water) and 0.7 g of water. Polymerization was performed in a closed vessel at 60 °C for 48 h. After maturing of the geopolymer for one week, the geopolymeric monolith was ground. The particle size of the powdered geopolymer ranged between 5 and 50 μm.

A K, Ca-Geo-2 sample with potassium as a charge-compensating cation was prepared by mixing of 10 g metakaolin (43.5 wt.% of Al_2O_3 and 53.7 wt.% of SiO_2) and 8 g of grinding granulated blast furnace slag with 16.2 g of potassium water glass (18.3 wt.% of SiO_2, 17.3 wt.% of K_2O; molar ratio SiO_2/K_2O of 1.7). Polymerization was performed in a closed vessel at RT. After maturing of the geopolymer for four weeks, the geopolymeric monolith was ground. The particle size of the powdered geopolymer ranged between 5 and 50 μm.

The NH_4^+ form of the Geo-1 and Geo-2 geopolymers was obtained by an ion-exchange procedure with an aqueous 0.5 M NH_4NO_3 solution at RT (100 ml of solution per 1 g of geopolymer applied thrice over 12 h).

$CuNH_4$-Geo-1 and $CuNH_4$-Geo-2 geopolymer catalysts were prepared by the ion exchange of the corresponding parent geopolymer in the NH_4^+ cationic form with aqueous 0.1 M $Cu(NO_3)_2$ solution at RT for 24 h.

$CoNH_4$-Geo-2 geopolymer catalysts were prepared by equilibration of the corresponding parent geopolymer in the NH_4^+ cationic form with aqueous 0.1 M $Co(NO_3)_2$ solution at RT for 24 h. After each ion exchange procedure, all samples were carefully washed with distilled water and dried in the open air.

FeKCa-Geo-2 geopolymer catalyst was prepared using an impregnation procedure with a solution of $FeCl_3$ in acetyl acetone. The procedure is commonly used for preparation of Fe-zeolites yielding highly dispersed iron species. Details of the procedure are described in Refs. [14,15].

$PtNH_4$-Geo-2 catalyst was obtained by adding 100 ml of 2% $Pt[(NH_3)_4Cl_2]$ aqueous solution to a suspension of 1 g NH_4-Geo-2 in 100 ml H_2O. The mixture was stirred for 24 h, filtered, dried in the open air at RT and calcinated in an air stream at 450 °C.

The chemical composition of parent geopolymers and geopolymer catalysts determined by XFS is listed in Table 2.

2.2. Structural analysis of geopolymer catalysts

The amorphous nature of the samples was checked by X-ray powder diffraction analysis on a Philips MPD 1880 diffractometer with CuKα radiation in the Bragg–Brenato geometry and equipped with a graphite monochromator and scintillation counter. The X-ray pattern was measured in the region of 5–75° of 2θ with a 0.04° step.

The ATR FTIR spectroscopy technique was used to monitor the degree of networking of the geopolymers. The spectra were recorded on a Nicolet Protégé 460 FTIR spectrometer equipped with an MCT/A detector.

Transformation of metakaolin to a geopolymer was monitored by ^{27}Al MAS NMR spectroscopy. ^{27}Al MAS NMR experiments were carried out using a Bruker Avance 500 MHz (11.7 T) Wide bore spectrometer with 4 mm o.d. ZrO_2 rotors with a rotation speed of 12 kHz. High-power decoupling pulse sequences with $\pi/12$ (0.7 μs) excitation pulse were employed to collect ^{27}Al MAS NMR single pulse spectra. The ^{27}Al NMR observed chemical shift was referred to an aqueous solution of $Al(NO_3)_3$.

UV–Vis–NIR diffuse–reflectance spectra of hydrated parent and Co-, Cu- and Fe-geopolymers were collected in the range 200–2500 mm using Perkin–Elmer Lambda 950 spectrometer with Spectralon^{TM} integration sphere. Spectralon^{TM} served also as a reference. Grained samples were placed in a 5 mm thick optical quartz cell. Spectra were recalculated using the Kubelka–Munk equation: $F(R_\infty) = (1 - R_\infty)^2/2R_\infty$. For details see Refs. [10,16].

The size of the geopolymer particles was estimated from micrographs obtained with a scanning electron microscope Jeol (JSM-03).

Nitrogen sorption isotherms of parent geopolymers were measured with a ASAP 2020 (Micromeritics Instrument Corporation, Norcross, USA) volumetric instrument at −196 °C. Prior to the sorption measurements, all the samples were degassed at 250 °C for at least 24 h until a pressure of 10^{-3} Pa was attained.

The chemical compositions of parent geopolymers and geopolymers catalysts were determined by XFS with a Philips PW 1404 spectrometer, equipped with the UniQuant analytic program yielding semi-quantitative analysis of 74 elements from fluorine to uranium with 10% standard deviation.

2.3. Catalytic experiments

2.3.1. Total oxidation of hydrocarbons

Partial pressure saturators and mass flow controllers were used for feeding decane vapors and oxygen into a stream of He. The feed contained 250 ppm of n-decane, 6% O_2 and He as a carrier gas. An amount of 100 mg of catalysts of particle size of 0.3–0.5 mm

Table 2
Chemical composition of parent geopolymers and geopolymer catalysts.

Sample	PtO_2 (wt.%)	CuO (wt.%)	Co_3O_4 (wt.%)	Na_2O (wt.%)	K_2O (wt.%)	CaO (wt.%)	MgO (wt.%)	Al_2O_3 (wt.%)	SiO_2 (wt.%)	TiO_2 (wt.%)	Fe_2O_3 (wt.%)	H_2O (wt.%)
Na-Geo-1	–	–	–	13.0	0.50	0.17	0.14	19.5	43.1	0.16	0.23	23.2
NH_4-Geo-1	–	–	–	3.38	0.35	0.18	0.15	23.2	51.0	0.17	0.19	21.40
$CuNH_4$-Geo-1	–	11.62	–	0.23	0.34	0.19	0.13	22.4	49.5	0.17	0.18	15.24
KCa-Geo-2	–	–	–	0.47	12.5	13.1	2.18	19.8	42.5	0.86	0.74	7.8
NH_4-Geo-2	–	–	–	0.04	4.5	10.8	2.09	19.2	41.8	0.84	0.76	19.9
$CuNH_4$-Geo-2	–	21.9	–	0	1.41	2.98	1.53	20.9	45.2	0.96	0.95	4.53
$PtNH_4$-Geo-2	2.41	–	–	0.06	3.79	11.6	2.44	21.2	48.8	0.95	0.80	8.0
FeKCa-Geo-2	–	–	–	0.40	10.77	11.25	1.92	15.19	35.98	0.76	1.79	11.35
$CoNH_4$-Geo-2	–	–	11.6	0	2.71	2.1	1.91	20.3	44.8	0.93	0.82	14.83

and total flow rate of 100 ml min^{-1} corresponded to a GHSV of 60 000 h^{-1}. The concentrations of O_2, CO, CO_2 and hydrocarbons were determined by an on-line connected Hewlett–Packard 6890 gas chromatograph. Two gaseous samples were injected with two 10-port valves. Columns of Poraplot Q and molecular sieve 5A and a thermal conductivity detector (TCD) were used to separate and detect O_2, CO and CO_2. A Poraplot Q column separated CO_2 from O_2 and traces of N_2 and CO, and a six-port valve was used to bypass the column with molecular sieve 5A during the analysis of CO_2. In the second branch, hydrocarbons were separated on a Poraplot Q column and detected by FID. Details of the analysis have been described elsewhere [17].

2.3.2. Selective catalytic reduction of NO_x by NH_3

A fixed-bed flow-through quartz microreactor was used to analyse the activity of geopolymer catalysts in NH_3–SCR–NO_x. The composition of gases at the inlet of the reactor was typically 500 ppm NO and 500 NO_2, 2.5 O_2, and 1000 ppm NH_3 and He as a carrier gas. The weight of the catalyst (0.3–0.5 mm grains) was 50 mg, and the flow rate was 350 cm^3 min^{-1}, corresponding to a GHSV of 210 000 h^{-1}. All the gas connections were kept at a temperature of 200 °C to avoid the formation and deposition of NH_4NO_3. The concentrations of NO, NO_2 and NH_3 were monitored with a NO/NO_x/NH_3 analyzer (ABB Limas 11). The concentrations of N_2 and N_2O were determined by an on-line connected Hewlett–Packard 6890 gas chromatograph. Columns of Poraplot Q and molecular sieve 5A were used for the separation and TCD for the detection. Catalytic activities of geopolymers catalysts were compared with a commercial sample of commonly used V_2O_5/Al_2O_3 catalyst (Euro Support Manufacturing Czechia, CR).

3. Results and discussion

3.1. Synthesis and structure of geopolymers

The XRD patterns of the powdered Na-Geo-1 and KCa-Geo-2 samples are depicted in Fig. 1. The XRD patterns with a diffuse halo peak at about $2\theta = 30°$ indicates that the prepared samples are amorphous and contain only traces of crystalline compounds. This is in accordance with X-ray amorphous character of practically all poly(sialate-siloxo) and higher sialates resulting from polycondensation of alkali-alumino-silicates [8]. The traces of crystalline compounds are reflected in the XRD pattern of Na-Geo-1 kaolin by a weak sharp signal at $2\theta = 19.8$, quartz is manifested by sharp signals at $2\theta = 26.6°$, mullite by weak sharp signals at $2\theta = 16.4$, 25.4, 35.2, 39.4, 40.9, 42.7 and 60.7° and magnetite by a weak signal at $2\theta = 33.2°$. All these crystalline impurities were derived from the metakaolin used for preparation of both geopolymer samples. In the XRD pattern of KCa-Geo-2, kaolin is manifested by a weak signal at $2\theta = 19.8$, quartz by weak signals at $2\theta = 26.6°$, calcite by sharp signals at $2\theta = 29.4$ and merwinite ($Ca_3Mg(SiO)_4$), by a number of sharp signals at $2\theta = 32.5$, 33.4, 33,8, 39.5, 40.8, 41.7, 43.3, 44.6, 47.6, 48.5 and 60.4°. Merwinite and calcite are crystalline parts of granulated blast furnace slag used for preparation of the KCa-Geo-2 geopolymer.

Fig. 2 depicts the FTIR spectra of NH_4-Geo-1 and NH_4-Geo-2 geopolymers in the region of the T–O–T vibration. Three absorption bands typical of the geopolymer material were observed in the spectra at 870, 995 and 1120 cm^{-1}. The bands with maxima at 995 cm^{-1} (low frequency – LF band) and 1120 cm^{-1} (high frequency – HF band) are ascribed to the antisymmetric T–O–T vibration [10,18–21]. The ratio of the low and high frequency bands (LF/HF) can be used for rough estimation of the degree of polymerization of the geopolymer network [21]. The LF/HF ratios of 4.1 and 3.7 for NH_4-Geo-1 and NH_4-Geo-2, respectively, indicate a high degree of

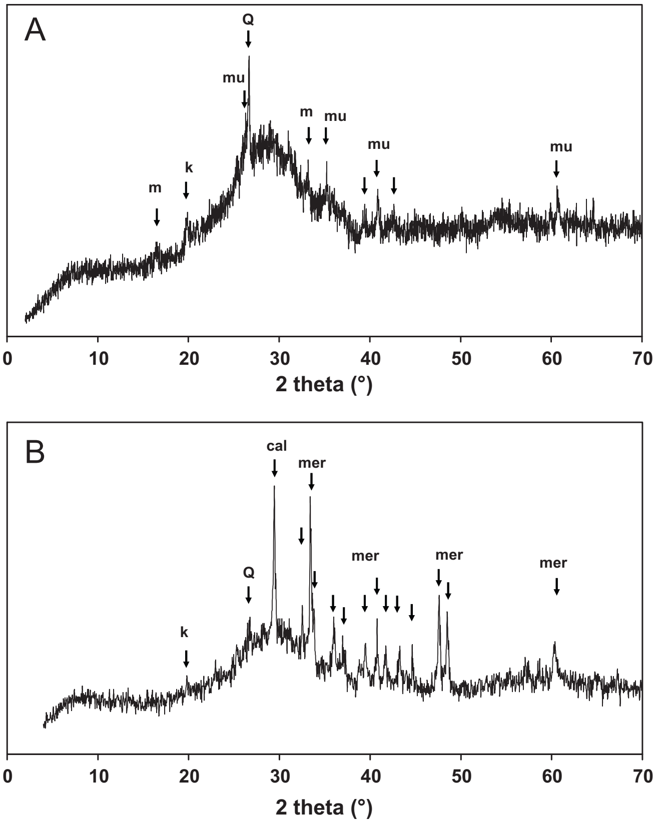

Fig. 1. X-ray diffraction pattern of Na-Geo-1 (A), KCa-Geo-2 (B). k, kaolin; Q, quartz; mu, mullite; m, magnetite, cal, calcite; mer, merwinite.

polymerization. The band at 873 cm^{-1} reflects the Si–OH bending vibration [18].

The ^{27}Al MAS NMR spectra of the Na-Geo-1 and KCa-Geo-2 samples are depicted in Fig. 3 and compared with the spectrum of the metakaolin used for their preparation. The resonance at 58 ppm corresponds to tetrahedrally coordinated Al atom and dominates spectra of both geopolymers. The resonance at 3 ppm can be ascribed to octahedrally coordinated Al of residual unreacted metakaolin and represents less than 4% of all the Al atoms. This indicates nearly complete transformation of metakaolin to the geopolymers.

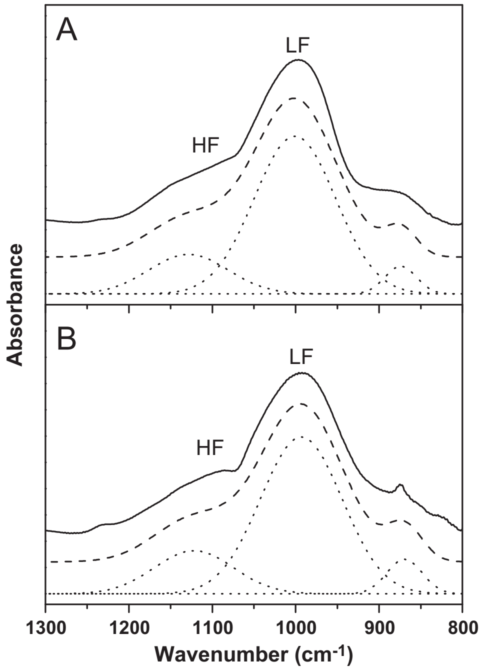

Fig. 2. ATR FTIR spectra of NH_4-Geo-1 (A) and NH_4-Geo-2 (B) geopolymers. Experimental spectrum (—), simulated spectrum (- - -), and its decomposition to individual Gaussian bands (. . .).

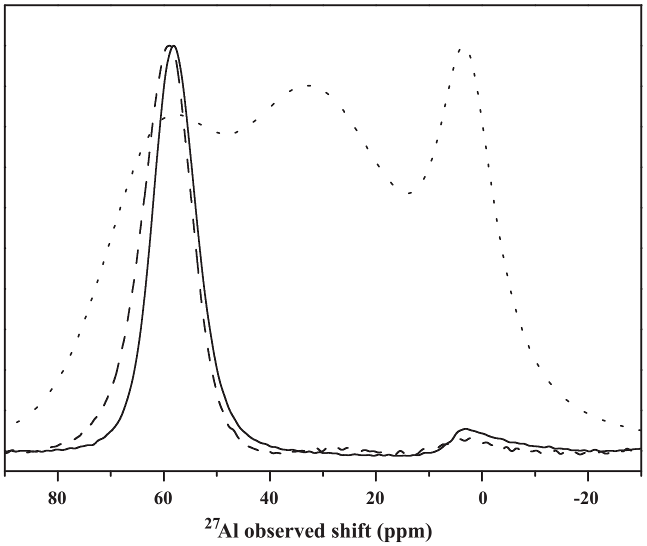

Fig. 3. ^{27}Al MAS NMR spectra of Na-Geo-1 (—), KCa-Geo-2 (- - -) and metakaolin used for geopolymer synthesis (. . .).

Surface area calculated by the BET method, pore volume obtained by BJH and *t*-plot methods and the pore diameters of the synthesised parent geopolymers are summarised in Table 3. It is shown that the synthesis yielded mesoporous parent geopolymers with mesopore volume of 0.089 and 0.095 $cm^3\,g^{-1}$ for Na-Geo-1 and KCa-Geo-2, respectively, and negligible microporosity (see Fig. 4 and Table 3). The observed mesoporosity is in good agreement with the results reported by Kriven, who observed that the geopolymer material consists of nanoparticulates ranging from 5 to 15 nm, separated by nanopores of 3 to 10 nm [9]. The maximum range of the pore size (10 and 8 nm for Na-Geo-1 and KCa-Geo-2) indicates that geopolymer-based catalysts can be able to accommodate spacious reactants or intermediates. In contrast to the synthesis of very compact geopolymer materials, which leads to the formation of materials of low porosity and surface area [22–25], the procedures employed in this study yield material with textural properties possibly usable for catalytically active material.

3.2. Active structures in geopolymer catalysts

The strategy for preparation of geopolymer materials with potential catalytic properties was based on close similarities of the interaction of cationic species of transient metals with geopolymers network and zeolites framework. An attempt was made to incorporate metal/metal–oxo cationic species into parent geopolymers to form similar structures, which provide high catalytic activity in

Table 3
Textural properties of parent geopolymers.

Sample	S_{BET} ($m^2\,g^{-1}$)	V_{BJH} ($cm^3\,g^{-1}$)	V_{Mi} ($cm^3\,g^{-1}$)	D (nm)	D_{max} (nm)
Na-Geo-1	17.1	0.089	0.0032	8–12	10
KCa-Geo-2	31.6	0.095	0	6–10	8

S_{BET} – surface area, V_{BJH} – mezopore volume, calculated by the BJH method, V_{Mi} – micropore volume determined by the *t*-plot method, D – pore size range, D_{max} – maximum of the pore size range.

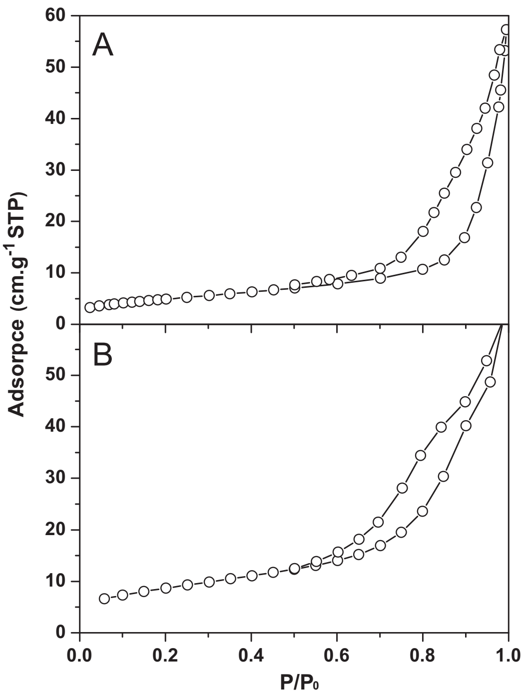

Fig. 4. Nitrogen adsorption isotherms of Na-Geo-1 (A) and KCa-Geo-2 (B).

redox reactions in zeolite based catalysts. Transition metals species (Cu, Co, Fe) and platinum as catalytic components providing high catalytic activity in commercial catalysts for catalytic reduction of nitrogen oxides by ammonia (NH_3–SCR–NO_x) and catalytic oxidation of VOC were used. Because geopolymer network exhibits the similarities with the zeolite framework in relation to ion exchange and accommodation of metal ions, mainly ion exchange procedures were employed for incorporation of cationic species into the parent geopolymers.

Divalent Cu(II) cationic species exhibit high activity and selectivity in NH_3–SCR–NO_x over Cu-zeolite based catalysts [26]. Cu was introduced into Na-Geo-1 and KCa-Geo-2 by a common ion-exchange with Cu(II) nitrate. It has recently been reported [10] that the internal volume of an originally sodium geopolymer can easily communicate with the external environment of the geopolymer and, thus, all extra-framework cations balancing the negative charge of the geopolymer network can be ion-exchanged by different ones. It is clear from the chemical analysis (see Table 2) that, using the ion exchange procedures, almost 98% of the Na^+ was exchanged with Cu^{2+} and $NH_4{}^+$ ions at $CuNH_4$-Geo-1 and 80% and 90% of Ca^{2+} and K^+, respectively, were exchanged at $CuNH_4$-Geo-2. Both Cu-geopolymers exhibited a blue colour, originated from a broad absorption band at the Vis–NIR spectra with a maximum between 12 000 and 13 500 cm^{-1} (shown in Fig. 5A), similar to the spectra of hydrated Cu-zeolites [27]. The octahedral or bipyramidal complexes of solvated Cu^{2+} ions with six or five water molecules can be attributed to this absorption [27]. Shift of the maximum and in the high energy edge to higher wavenumbers of the broad Cu^{2+} band in the spectrum of $CuNH_4$-Geo-2 compare to $CuNH_4$-Geo-1 indicates higher relative concentration of the $[Cu^{2+}X^-(H_2O)_5]^+$ complexes [27] in $CuNH_4$-Geo-2. The band at 32 000; 40 000 and 45 000 cm^{-1} can be assigned to $0^{2-} \rightarrow Cu^{2+}$ charge transfer (CT) transition [27]. The similar intensity of the bands of d–d transition of Cu^{2+} ions for both Cu-geopolymers and significantly higher intensity of the charge transfer bands for $CuNH_4$-Geo-2 can be explained by different extinction coefficients of $[Cu^{2+}(H_2O)_6]^{2+}$ and $[Cu^{2+}X^-(H_2O)_5]^+$ complexes present in ion exchanged samples. It follows that the ion-exchange procedure of geopolymers provided predominantly Cu^{2+} ions located at cationic sites and balancing two or one negative charge of the geopolymer network.

Co and Fe species are typical components of catalysts based on supported noble metals or oxides of transition metals for total oxidation of VOC [28,29]. The common ion-exchange procedure employed to prepare $CoNH_4$-Geo-2 led analogously to $CuNH_4$-Geo-2 to ion-exchange of 80% and 85% of Ca^{2+} and K^+, respectively, by Co^{2+} and $NH_4{}^+$ ions, as indicated by the chemical analysis. Co-geopolymer is lightly pink coloured, as observed from UV–Vis spectra (Fig. 5B) due to the absorption band around 19 000 cm^{-1} typical for octahedral Co(II) hexaquo-complexes [30,31]. The bands in UV region above 40 000 cm^{-1} correspond to the $0^{2-} \rightarrow Co^{2+}$ CT transitions well known for hydrated Co-zeolites [31]. Thus extra-network solvated $[Co^{2+}(H_2O)_6]^{2+}$ complexes balance network Al negative charge in Co-geopolymer. Details of structural analysis of the Co species in geopolymer materials including the dehydrated UV–Vis spectra, which indicate the presence of three types

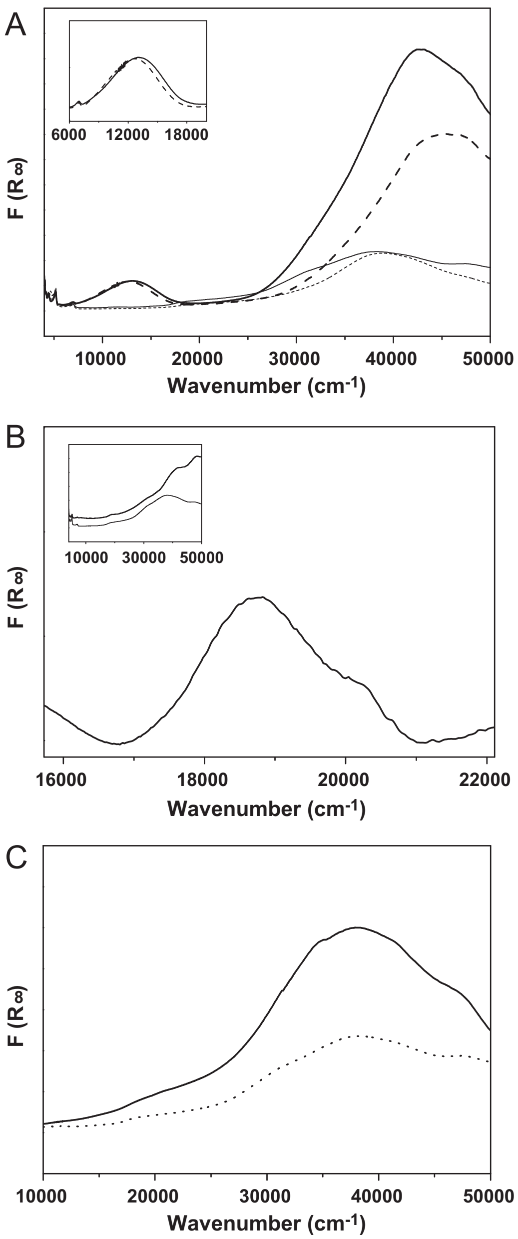

Fig. 5. DR UV–Vis–NIR spectra of geopolymer catalysts. (A) $CuNH_4$-Geo-2 (—), $CuNH_4$-Geo-1 (- - -), NH_4-Geo-2 (—) and NH_4-Geo-1 (. . .) (B) $CoNH_4$-Geo-2 (—). (C) FeKCa-Geo-2 (—) and NH_4-Geo-2 (. . .).

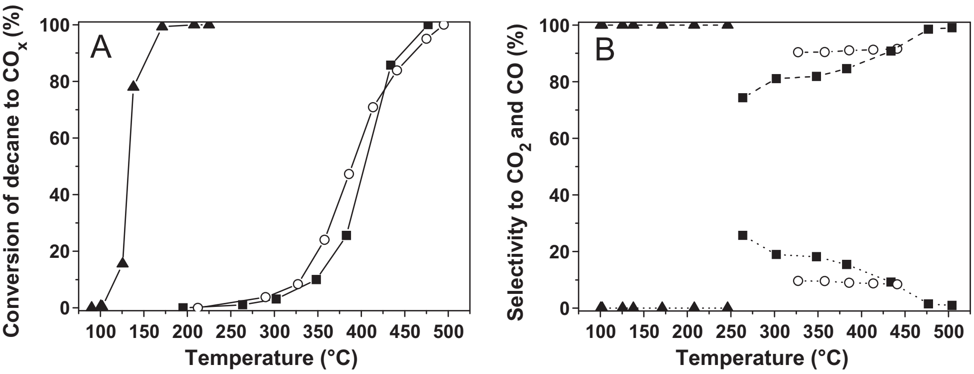

Fig. 6. Conversion of decane (A) and selectivity for CO_2 (dash line) and CO (dot line) (B) at total oxidation as a function of the temperature over $PtNH_4$-Geo-2 (▲), FeKCa-Geo-2 (○) and $CoNH_4$-Geo-2 (■). GHSV = 60 000 h^{-1}, 250 ppm decane and 6% O_2 in a He stream.

of well-defined local structures accommodating Co^{2+} ions in local arrangement similar to those in Si rich zeolites have been published elsewhere [10].

The impregnation method employing $FeCl_3$ + ACAC mixture was used for preparation of Fe-geopolymer, because it is well-known for providing highly dispersed Fe-ions species with limited formation of Fe-oxo species in zeolites [32]. UV–Vis spectra of $FeNH_4$-Geo-2 and the corresponding parent geopolymer are shown in Fig. 5C. Already in the spectrum of parent geopolymer a doublet of small intensity at 11 000 and 11 800 cm^{-1} corresponding to the $^6A_{1g} \rightarrow {}^4T_{1g}(^4G), {}^4T_{2g}(^4G)$ d–d transitions of Fe(III) ion in an octahedral environment of oxygen-containing ligands [33] and absorption edge at about 18 500 cm^{-1} corresponding to the d–d electron pair transition [33] were observed. These bands were unambiguously assigned to hematite. The high energy bands at about 33 000, 38 000 and 46 000 cm^{-1} were ascribed to non-specific $0^{2-} \rightarrow Fe^{3+}$ charge transition transfer. Thus already small amount of Fe-oxide coming from metakaolin used for preparation is present in the parent geopolymer, cf. chemical analysis of prepared geopolymers. UV–Vis spectrum of $FeNH_4$-Geo-2 shows significant increase of the intensity of the CT bands at about 33 000, 38 000 and 46 000 cm^{-1}, not followed by corresponding increase of the absorption edge around 18 000 cm^{-1} associated with Fe-oxides. This indicates formation of highly dispersed Fe species most likely in the form of Fe(III) complexes – $[Fe(H_2O)_6]^{3+}$, $[Fe(H_2O)_5(OH)]^{2+}$ and $[Fe(H_2O)_4(OH)_2]^+$ in as prepared sample. Thus the impregnation provided distribution of Fe species in Fe-geopolymer similar to obtained for zeolites, cf. for instance structure of Fe species in ZSM-5 and beta zeolite in Ref. [33].

Impregnation with $Pt[(NH_3)_4Cl_2]$ solution with subsequent calcination should provide clusters of platinum species of undefined sizes. Analysis of these structures by UV–Vis–NIR spectroscopy is limited due to the presence of Fe species in parent geopolymer.

3.3. Geopolymers in redox catalysis

3.3.1. Total oxidation of VOC

Decane is one of the major components of diesel fuel and auto motive transport represents one of the most important sources of VOC pollution [34]. Therefore it was used as a model compound for the test of total oxidation of VOC over geopolymer catalyst. Conversion of decane and selectivity for CO_2 and CO in the total oxidation of decane as a function of temperature over $PtNH_4$-Geo-2, FeKCa-Geo-2 and $CoNH_4$-Geo-2 catalysts is shown in Fig. 6. The reactions were carried out at an oxygen concentration of 6%, i.e., lower oxygen concentration than in the air, which is typical for exhaust gases of combustion processes. $PtNH_4$-Geo-2 already exhibits high conversion at very low temperatures with 50% conversion of decane obtained at 135 °C. The oxidation is highly selective for CO_2 whereas CO has not been detected in the products of combustion even at temperatures of approx. 100 °C and oxygen concentration of 6%. The working temperature window for both FeKCa-Geo-2 and $CoNH_4$-Geo-2 catalysts is understandably shifted to higher temperatures than for the Pt-geopolymer. The reaction starts at 260 °C and total conversion is achieved at 470–480 °C. The selectivity for CO_2 exhibits an increasing tendency with increasing temperature when CO is completely oxidised to CO_2 at 470 °C over $CoNH_4$-Geo-2. Thus both Fe and Co located in geopolymer in the form of atomically dispersed extra-network cationic species balanced by network negative charge catalyse the oxidation reaction in middle temperatures for total oxidation of VOC. Pt species in geopolymer exhibit high catalytic activity already at very low temperatures. Thus the high conversions achieved with decane at low and medium temperatures, together with the high thermal stability of the geopolymers, exemplified the possible potential for utilization of geopolymer catalysts in total oxidation of VOC.

3.3.2. Activity of geopolymer catalysts in NH_3–SCR–NO_x

The NO_x and NH_3 conversions in the NH_3–SCR–NO_x reaction as a function of reaction temperature for Cu-geopolymers, NH_4-geopolymer and commercial V_2O_5/Al_2O_3 catalyst are compared in Fig. 7. For NH_4-Geo-1, the NO_x and NH_3 conversion began at 300 °C and increased with increasing reaction temperature. The activity is essentially related to the presence of acid sites important for adsorption of basic molecules of ammonia and traces of transition metals most likely Fe involved in the redox cycle. The introduction of Cu into the NH_4-Geo-1 geopolymer resulted in markedly improved catalyst activity over the entire temperature range. $CuNH_4$-Geo-1 exhibits significant conversion of NO_x already at 250 °C and this increase with the reaction temperature, passing through a maximum at 400 °C and then declining slightly. The important observation is that NH_3 is completely oxidised already at a temperature of 230 °C and no NH_3 slip is present above this temperature. It follows that Cu^{2+} ionic species located at cationic sites of geopolymer network catalyses the NH_3–SCR–NO_x reaction already at low temperatures and preserves the process from NH_3 slip. The conversion of NO_x was already observed for $CuNH_4$-Geo-2 containing a high amount of copper at temperatures below 200 °C; however, then the conversion of NO_x declined at temperatures above 250 °C due to the lack of non-selective oxidised NH_3 by O_2, as is indicated by the steadily increasing conversion of NH_3. The non-selective consumption can be related to the formation of low dispersed Cu-oxide like species present in higher concentration in $CuNH_4$-Geo-2. Such species could be formed upon catalytic test from $[Cu^{2+}X^-(H_2O)_5]^+$ complexes balancing one negative charge of the network. In dehydrated geopolymer under oxidative atmosphere, bare Cu^{2+} ion should be balanced by neg-

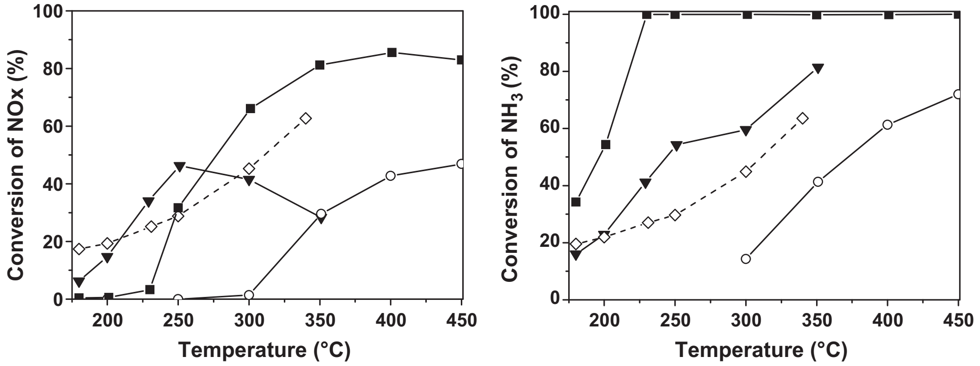

Fig. 7. Conversion of NO_x and NH_3 to nitrogen as a function of temperature at NH_3–SCR–NO_x over (□) NH_4-Geo-1, (■) NH_4Cu-Geo-1, NH_4Cu-Geo-2 (▼) and V_2O_5/Al_2O_3 (◊) catalysts. Conditions: 500 ppm NO, 500 ppm NO_2, 1000 ppm NH_3 and 2.5% O_2 in a He stream, GHSV = 210 000 h^{-1}.

ative charge of the network formed from two Al atoms. Thus the formation of Cu-oxide like species occurs from over-stoichiometric Cu^{2+} ions similarly to Cu-zeolite catalysts [35,36]. The conversion of NO_x and NH_3 obtained over geopolymer catalysts is compared with a commercial sample of commonly used V_2O_5/Al_2O_3 catalyst. V_2O_5/Al_2O_3 exhibits slightly increasing conversion of NO_x and NH_3 with increasing temperature and highly selective utilization of NH_3. The high selectivity resulted in a high ammonia slip. From comparison of conversions of NO_x obtained for geopolymer and the commercial catalysts, it is clear that $CuNH_4$-Geo-1 could compete with the common catalyst in the temperatures range of 250–350 °C. The higher conversion of NH_3 over $CuNH_4$-Geo-1 compared to the V_2O_5/Al_2O_3 catalyst can be advantageous in processes with limited possibility of precise dosing of NH_3 into the deNO_x process; however, it can slightly decrease utilization of NH_3 under steady-state conditions.

It has to be noticed that results presented in this study represents very first attempt to investigate catalytic properties of geopolymer based materials. The geopolymers are traditionally applied in other fields with requirements on geopolymer properties opposite to those advantageous for catalytic applications [22–25]. On the other hand, preparation of geopolymer materials is simple and low cost and results in material with high thermal stability [2,8]. Moreover, easy fabrication of geopolymer monolithic material posses the possibility to prepare geopolymer monolith in forms suitable for catalytic application [37]. Thus, significant improvements of geopolymer catalysts properties can be supposed to achieve in such areas as surface area of catalyst, hierarchical arrangement of macro- and meso-pores and local arrangement of structures accommodating active species by understanding of geopolymer synthesis. Further improvement can be obtained by understanding of the relationship between geopolymer local structure, properties of incorporated metal ion species and catalytic performance of geopolymer based catalyst.

4. Conclusions

Transition metal ions and rare metal species balancing network negative charge can be located in extra-network positions of the geopolymer. The extra-network species can be introduced by simple procedures as it is ion-exchange or impregnation. Extra-network transition metal ions and Pt species located in geopolymer exhibit redox properties and, thus, functionalized geopolymers possess catalytic properties in heterogeneously catalysed redox reactions. The redox catalytic properties of the Pt, Fe, Cu and Co geopolymer catalysts were demonstrated on NH_3–SCR–NO_x by ammonia and total oxidation of volatile hydrocarbons. Reached conversion of NO_x to nitrogen and decane to CO_2 indicate potential of studies on geopolymers based catalytic materials.

Acknowledgement

Financial support was provided through project # FT-TA4/068 of Ministry of Industry and Trade of the Czech Republic and project # KAN100400702 of the Academy of Sciences of the Czech Republic. This study was performed within the EU Network of Excellence IDECAT #NMP 3-CT-2005-011730.

References

[1] J. Davidovits, Journal of Thermal Analysis 37 (1991) 1633–1656.
[2] J. Davidovits, M. Davidovics, Geopolymer. Ultra-high temperature tooling material for the manufacture of advanced composites, in: International SAMPE Symposium and Exhibition (Proceedings), pt. 2 ed., 1991, pp. 1939–1949.
[3] US patent 4509985 (1985).
[4] J.G.S. Van Jaarsveld, J.S.J. Van Deventer, L. Lorenzen, Metallurgical and Materials Transactions B: Process Metallurgy and Materials Processing Science 29 (1998) 283–291.
[5] US patent 4859367 (1989).
[6] R.E. Lyon, P.N. Balaguru, A. Foden, U. Sorathia, J. Davidovits, M. Davidovics, Fire and Materials 21 (1997) 67–73.
[7] L. Li, S.B. Wang, Z.H. Zhu, Journal of Colloid and Interface Science 300 (2006) 52–59.
[8] J. Davidovits, Geopolymer Chemistry and Application, 3rd printing, Institute Geopolymer, Saint Quentin, France, 2008, pp. 20–36.
[9] W.M. Kriven, J.L. Bell, M. Gordon, Ceramic Transactions 153 (2003) 227.
[10] O. Bortnovsky, J. Dedeček, Z. Tvarůžková, Z. Sobalík, J. Šubrt, Journal of the American Ceramic Society 91 (2008) 3052–3057.
[11] Z. Liu, S. Ihl Woo, Catalysis Reviews – Science and Engineering 48 (2006) 43–89.
[12] Patent pending PV 2009-240.
[13] CZ patent 301936 (2010).
[14] CZ patent 293917 B6 (2001).
[15] N.K. Sathu, P. Sazama, V. Valtchev, B. Bernauer, Z. Sobalik, Oxidative dehydrogenation of propane over Fe-BEA catalysts, Studies in Surface Science and Catalysis (2008) 1127–1130.
[16] J. Dedecek, B. Wichterlova, Journal of Physical Chemistry B 103 (1999) 1462–1476.
[17] P. Sazama, L. Čapek, H. Drobná, Z. Sobalík, J. Dědeček, K. Arve, B. Wichterlová, Journal of Catalysis 232 (2005) 302–317.
[18] V.F.F. Barbosa, K.J.D. MacKenzie, C. Thaumaturgo, International Journal of Inorganic Materials 2 (2000) 309–317.
[19] J.L. Provis, G.C. Lukey, J.S.J. Van Deventer, Chemistry of Materials 17 (2005) 3075–3085.
[20] G. Coudurier, C. Naccache, J.C. Vedrine, Journal of the Chemical Society, Chemical Communications (1982) 1413–1415.
[21] O. Bortnovsky, Z. Sobalík, Z. Tvarůžková, J. Dědeček, P. Roubíček, Z. Prudková, M. Svoboda, in: J. Davidovits (Ed.), Geopolymers, green chemistry and sustainable development solutions, Proceedings of Geopolymer 2005 World Congress, Saint-Quentin, France, 2005, pp. 81–84.
[22] J.L. Provis, P. Duxson, J.S.J. van Deventer, Advanced Powder Technology 21 (2010) 2–7.
[23] F. Svara, P. Svoboda, J. Dolezal, Z. Bittnar, V. Smilauer, L. Kopecky, R. Sulc, Ceramics – Silikaty 52 (2008) 296–298.
[24] B.V. Rangan, Indian Concrete Journal 82 (2008) 7–15.
[25] P. Duxson, J.L. Provis, Journal of the American Ceramic Society 91 (2008) 3864–3869.
[26] S. Kieger, G. Delahay, B. Coq, B. Neveu, Journal of Catalysis 183 (1999) 267–280.
[27] J. Dedecek, B. Wichterlova, Journal of Physical Chemistry B 101 (1997) 10233–10240.

[28] S.C. Kim, Journal of Hazardous Materials 91 (2002) 285–299.
[29] J.M. Giraudon, A. Elhachimi, G. Leclercq, Applied Catalysis B: Environmental 84 (2008) 251–261.
[30] J. Dedecek, L. Capek, D. Kaucky, Z. Sobalik, B. Wichterlova, Journal of Catalysis 211 (2002) 198–207.
[31] L. Capek, J. Dedecek, P. Sazama, B. Wichterlová, Journal of Catalysis 272 (2010) 44–54.
[32] K. Jíša, J. Nováková, M. Schwarze, A. Vondrová, S. Sklenák, Z. Sobalík, Journal of Catalysis 262 (2009) 27–34.
[33] L. Capek, V. Kreibich, J. Dedecek, T. Grygar, B. Wichterlová, Z. Sobalík, J.A. Martens, R. Brosius, V. Tokarová, Microporous and Mesoporous Materials 80 (2005) 279–289.
[34] C. Badol, N. Locoge, J.C. Galloo, Science of the Total Environment 389 (2008) 429–440.
[35] J. Dedecek, L. Capek, B. Wichterlová, Applied Catalysis A: General 307 (2006) 156–164.
[36] B. Wichterlova, Z. Sobalik, J. Dedecek, Catalysis Today 38 (1997) 199–203.
[37] WO Patent 121823A2 (2006).